buildings

MDPI

Article

Analysis of Unsteady Heat Transfer during Ice-Making Process for Ice Rink Buildings

Shiqi Wang [1,2], Yumeng Wu [1], Paiwei Zhang [1], Meiyuan Yang [1,2], Zhenying Zhang [1,2,*] and Hongli Wang [3]

[1] Department of Architecture and Civil Engineering, North China University of Science and Technology, Tangshan 063210, China
[2] Tangshan Key Laboratory of Low-Carbon Built Environment, North China University of Science and Technology, Tangshan 063210, China
[3] Department of Metallurgy and Energy, North China University of Science and Technology, Tangshan 063210, China
* Correspondence: zzying@tju.edu.cn

Abstract: The ice-making process is an important factor that affects the ice quality and the energy consumption of ice rinks. An unsteady heat transfer model is established and validated for the ice-making process. The transient temperature variation and ice thickness growing characteristics during the ice-making process are analyzed. The freezing time of a water layer and the final temperature of the stabilized ice layer are quantified. The effects of ice rink structural parameters on the ice-making process are studied. The results show that the water temperature variations during the process go through three stages. The ice-growing process mainly occurs in the second stage. The ice-making process takes about 305 min–420 min for a water layer of 5 mm thickness. The reduction in the ice-making time and the decrease in the final temperature of the stabilized ice layer can be attained by reducing the water layer thickness, the surface heat flux, the cooling pipe spacing, the fluid temperature in the cooling pipe, or the top concrete thickness. Among them, the influences of the thickness of the water layer, the surface heat flux, and the fluid temperature in the cooling pipe are more significant. As the thickness of the water layer decreases from 7 mm to 3 mm, the total ice-making time decreases by about 37.6%. The ice-making time is reduced by 17.1% with the surface heat flux decreasing from 330 W/m^2 to 250 W/m^2. The ice-making time is reduced by 21.4% with the cooling pipe temperature decreasing from −15.5 °C to −19.5 °C.

Keywords: ice rink; heat transfer; ice-making; water layer; unsteady

check for updates

Citation: Wang, S.; Wu, Y.; Zhang, P.; Yang, M.; Zhang, Z.; Wang, H. Analysis of Unsteady Heat Transfer during Ice-Making Process for Ice Rink Buildings. *Buildings* **2023**, *13*, 291. https://doi.org/10.3390/buildings13020291

Academic Editor: Christopher Yu-Hang Chao

Received: 4 December 2022
Revised: 13 January 2023
Accepted: 15 January 2023
Published: 18 January 2023

Copyright: © 2023 by the authors. Licensee MDPI, Basel, Switzerland. This article is an open access article distributed under the terms and conditions of the Creative Commons Attribution (CC BY) license (https://creativecommons.org/licenses/by/4.0/).

1. Introduction

Ice rink buildings consume large amounts of energy for ice-making and maintenance. The average annual energy consumption of a typical ice rink is about 1500 MWh, and the maximum energy consumption can reach 2400 MWh [1,2]. The system of ice-making and maintenance accounts for 35–75% of the total energy consumption of the ice rink [3]. The ice quality of the ice rink is an important factor that affects the performance of competition events. The accurate prediction of the ice-making process is not only about whether the ice rink can meet the technical requirements of the game but is also related to the initial investment in the equipment and operating costs of the system. Therefore, analyzing the heat transfer and ice-making process of the ice rink plays a key role in its design and operation.

Many studies have simulated the heat transfer process of ice rinks. In 1986, Brown and Pearson [4] developed a mathematical model to investigate the influence of the cooling pipe diameter, ice layer thickness, concrete thickness, and pipe location in the concrete slab on ice surface temperature variation, as well as the refrigerant temperature required for different surface temperatures. In 2005, Bellache et al. [5,6] analyzed the heat and mass transfer load of ice rinks by establishing steady heat transfer models. In 2006, Mun

and Krarti [7] established a small-scale ice rink experimental device to evaluate the heat transfer performance of the ice rink under different insulation thermal resistances. The results showed that a temperature difference of 3 °C exists between the bottom corner and the center of the ice rink during the ice-freezing process, and the addition of a thermal insulation layer could decrease the cooling load, shorten the time for ice-making, and help maintain a lower average ice temperature. In 2008, Somrani et al. [8] established a simulation model including heat transfer under the floor to study the influence factors of cooling medium temperatures and thermal conductivity in the ice-freezing process. In 2010, Mun [9] established a small-scale ice rink model, using a sandy surface. The structure of the ice rink model is divided into three layers: a wood floor, a sandy surface layer (including copper pipes), and a water layer. A polystyrene insulation layer is located under the floor. In 2013, Coman et al. [10] conducted an experimental study on the temperature distribution around the cooling pipes and the quality of the ice around the pipes in an artificial ice rink by using finite element numerical simulation combined with experiments. The research results showed that the different temperature changes at the pipe wall and between the pipes led to rapid freezing near the pipes, while the freezing speed between the pipes was slow. In 2021, Zhou et al. [11] established an ice rink discrete thermal resistance circuit model and analyzed the influence of the distance between the cooling pipes on the ice under a steady-state condition. In 2022, Zhang et al. [12] performed a parametric analysis of the cooling pipes in an ice rink through a steady heat transfer approach, and the temperature of the working medium in the cooling pipe is suggested.

To sum up, many studies have studied the influence of ice rink parameters on the heat transfer performance in ice rinks through the steady approach. Nevertheless, the actual ice-making process of ice rinks is an unsteady heat and mass transfer process, which involves phase changing [13]. Significantly less literature is available on the transient ice-making process in the ice rink. In 2021, Li et al. [14] uses a double ethylene tetra fluoro ethylene membrane structure to reduce radiation heat transfer and ice surface heat flux, which reduces ice-making load by 7% and accelerates ice freezing. Li et al. [15] simulated and verified the heat and mass transfer changes in the process of ice-making, ice maintenance, and ice resurfacing in an artificial ice rink by establishing a model and considered steady and dynamic factors. The results showed that under the dynamic state, the mass transfer process would affect the duration and cooling load of the ice-making and ice-repairing process. In 2022, Li et al. [16] found that the humidity of the air around the ice surface affects the heat flux and freezing of the ice. Lin et al. [17] analyzed the influence of the air parameters affected by the enclosure structure on the mass transfer process during the ice-making process and found that air with low moisture content can reduce the heat flow on the ice surface and accelerate ice freezing. Unfortunately, the effect of ice rink structural parameters on the ice-making process has been ignored and not quantified in these investigations.

In this paper, the unsteady physical model and mathematical model of the ice-making process of an ice rink are established, and the unsteady heat transfer process with ice freezing in an artificial ice rink is studied. The transient temperature variation and ice thickness growing characteristics during the process are analyzed. The freezing time of the water layer is quantified, and a parametric analysis of the ice-making process is performed through the unsteady approach.

2. Materials and Methods

The ice-making process is an unsteady heat transfer process with a water–ice phase transition. In order to analyze the characteristics of the process, a coupling model of solid heat transfer and phase change fluid heat transfer in an ice rink with a water layer at the top was established by using COMSOL Multiphysics 5.6, and the transient state was studied.

The simulation procedure is as follows: at first, the physical model of the ice rink was built and drawn using the commercial software COMSOL. Afterward, the computational domain of the ice rink was determined. Then, the grids in each section of the ice rink were

meshed, and grid independence verification was implemented to ensure the dependability of the grid. Next, the model was built using the input values of the initial value of temperature and the boundary conditions to perform the calculations. Then, the model was validated. Finally, the calculation and post-processing were performed and the impact of different parameters of the ice rink on the time and temperature of the water layer freezing process was studied.

2.1. Heat Transfer Model of the Ice Rink

The ice rink structure is shown in Figure 1. It is composed of a water layer, an ice layer, a concrete layer with cooling pipes, an insulation layer, an antifreeze layer with antifreeze pipes, and the soil layer. The water layer is used to study the freezing process. The ice rink structure is referenced from the ice rink design guide of the International Ice Hockey Federation. Copper pipes are used as cooling pipes, and polyethylene pipes are used as antifreeze pipes. The materials and physical parameters of each structural layer are shown in Table 1, and the physical properties are determined according to the reference [18].

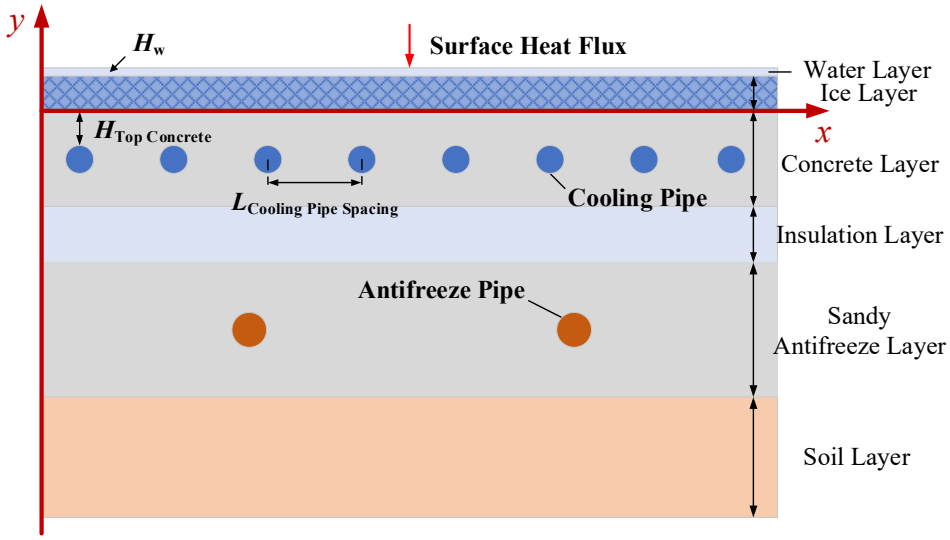


Figure 1. Structure of artificial ice rink.

Table 1. Thermophysical parameters and geometry of ice rink.

Layer	Thickness (mm)	Density (kg/m^3)	Specific Heat [J/(kg·°C)]	Thermal Conductivity [W/(m·K)]
Water	5	1000	4200	0.60
Ice	30	917	2090	2.21
Concrete	170	2500	840	1.63
Insulation	100	40	2100	0.034
Antifreeze	500	2650	1050	0.38
Soil	50	2000	1530	1.08

The ice-making process of the ice rink is a three-dimensional heat transfer problem. Because the temperature difference between the inlet and outlet of the cooling pipe is less than 2 °C, the heat transfer in the cooling pipe axial direction is neglected [13]. A 2D numerical model is established in this paper. The physical model of the ice rink is shown in Figure 1, where the water/ice layer, pipes, insulation layer, sandy layer, and soil layer are all considered. The 2D model was considered as a computational domain. The thermophysical and geometric parameters of the ice rink in COMSOL were set as in Table 1.

The control equation of transient heat transfer with phase transition is shown as [15]:

$$\rho C_p \frac{\partial T}{\partial t} = k\nabla^2 T + q_v \quad (1)$$

The main methods for calculating the latent heat process are the moving boundary method [19], the apparent heat capacity method [20], and the enthalpy method [21]. Here, the apparent heat capacity method is applied to calculate the water–ice phase transition. The analysis of water–ice phase transition process is shown in Figure 2. When the temperature of the water reaches $T_0 + 0.5\Delta T_{1\to2}$, the phase transition process starts, and the latent heat starts to be released. However, the temperature of the fluid stays constant. In the apparent heat capacity method, the change in enthalpy value is obtained by calculating the change in specific heat capacity during this period. At this $\Delta T_{1\to2}$ stage, water and ice occur smoothly, and the total heat released per unit volume is equal to the set latent heat value. When $T_0 - 0.5\Delta T_{1\to2}$, θ_i becomes 1, water is completely transformed into ice, and the release of latent heat ends; the specific heat capacity is also completely converted from the specific heat capacity of liquid water to the specific heat capacity of solid ice. The smaller the phase transition interval $\Delta T_{1\to2}$, the closer to the real process. However, the stability and convergence of the model will deteriorate. Therefore, 0.5 °C is selected for $\Delta T_{1\to2}$ according to the reference [20]. By introducing the assumed phase change temperature range, the heat capacity change process within this range is shown in Equation (2) [22,23]. The remaining thermal conductivity, density, thermal conductivity, and mass fraction are calculated according to the proportion of solid to liquid.

$$c_p = \frac{1}{\rho}\left(\theta_w \rho_w c_{p,w} + \theta_i \rho_i c_{p,i}\right) + l_{w\to i}\frac{\partial \alpha}{\partial T} \tag{2}$$

$$k = \theta_w k_w + \theta_i k_i \tag{3}$$

$$\rho = \theta_w \rho_w + \theta_i \rho_i \tag{4}$$

$$\alpha = \frac{1}{2}\frac{\theta_i \rho_i - \theta_w \rho_w}{\theta_i \rho_i + \theta_w \rho_w} \tag{5}$$

$$\theta_i + \theta_w = 1 \tag{6}$$

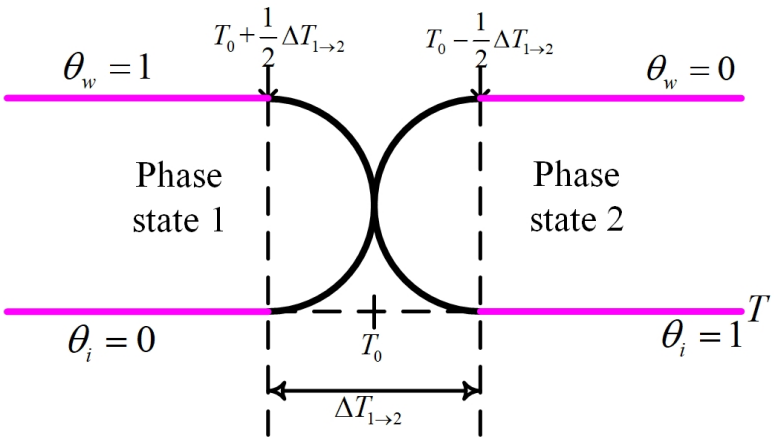


Figure 2. Schematic diagram of apparent heat capacity method.

2.2. Initial Conditions and Boundary Conditions

After establishing the ice rink model and setting the parameters, solid heat transfer and phase change fluid modules are introduced. By coupling the two calculation modules, transient calculation and analysis are carried out. To get as close as possible to the actual process of ice-making, the initial temperature of each layer of the ice rink is determined by steady-state simulation under the same model and boundary conditions. The calculation formula is as follows:

$$T_{\tau=0^-} = T_{steady} \tag{7}$$

The water layer surface boundary condition belongs to the second type. The heat flux on the water layer surface is determined by Lu [18]:

$$\frac{\partial T}{\partial n} = q_c \tag{8}$$

where n and q_c are the boundary normal and ice rink cooling load, respectively. The heat flux on the water layer surface is calculated according to Zhang et al. [12]. It is the sum of convection heat transfer flux between air and surface, condensation heat of water vapor in the air, radiation heat transfer between enclosure structures such as ceiling and ice surface, and the lighting load.

The mainstream temperature of the fluid in the cooling pipes is determined through the cooling load of the ice rink. The mainstream temperature of the fluid in the antifreeze pipes is determined by the references [18,22].

The research shows that the soil temperature in each city tends to be stable with the depth change. When the soil depth exceeds 10 m, the temperature of the soil is almost constant [24]. Therefore, the temperature at 10 m soil depth is set as 14.5 °C, which is obtained by the simulation of the authors [25].

Other boundary conditions are set as thermal insulation boundaries.

2.3. Grid Independence Verification

The size and shape of the grid affect the accuracy of the calculation results and the calculation time. The grid's partially enlarged view of the ice rink is shown in Figure 3. The free triangle grid is used for division, and the frozen water layer, cooling pipes, and antifreeze pipes are densified and refined. At the same time, three levels of cell size were selected for grid independence verification, and 5200, 79,000, and 690,000 grids were divided, respectively.

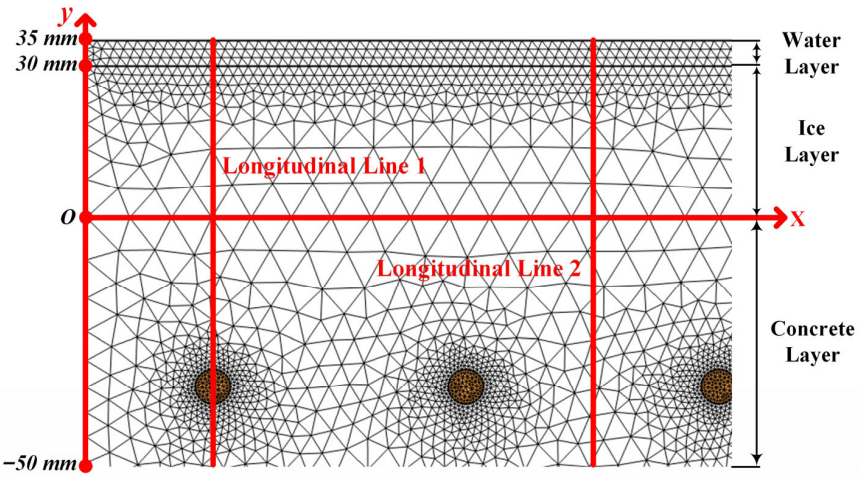


Figure 3. Local grid of ice rink.

In order to further verify the independence of the grid, the longitudinal line 1 (running through the cooling and antifreeze pipes at the same time) and the longitudinal line 2 (at the center of the cooling pipe spacing) in Figure 3 are selected to analyze the temperature distribution from the top of the ice surface to the last layer of the ice rink model, as shown in Figure 4. Under different grid numbers, both longitudinal lines 1 and 2 show a parabolic downward trend of temperature above the cooling pipes. Figure 4a decreases from about −3.2~−4.0 °C at the ice surface to −17.5 °C at the cooling pipe surface. The cooling pipe is set in the isothermal range, so the central temperature does not change; Figure 4b decreases from about −3.5~−4.1 °C at the ice surface to −13~−15 °C at the center of the distance between the cooling pipes. The 100 mm thick insulation layer can significantly eliminate the temperature from about −11 °C to about 6 °C. The sand layer set under the insulation

layer is arranged with antifreeze pipes to keep the temperature of the sand layer between 6 °C and 10 °C and prevent soil freezing. It can be seen that the grid number is 7200–64,000, and the calculated temperature error caused by the grid is relatively large. The temperature error can reach 1~2 °C, which is obviously not applicable. As the number of grids increases from 64,000 to 690,000, the temperature error decreases significantly, and the temperature distribution is almost the same. This shows that the number of grids has little impact on the results in this interval. Considering the calculation accuracy and time, 79,000 grids are finally selected in this paper.

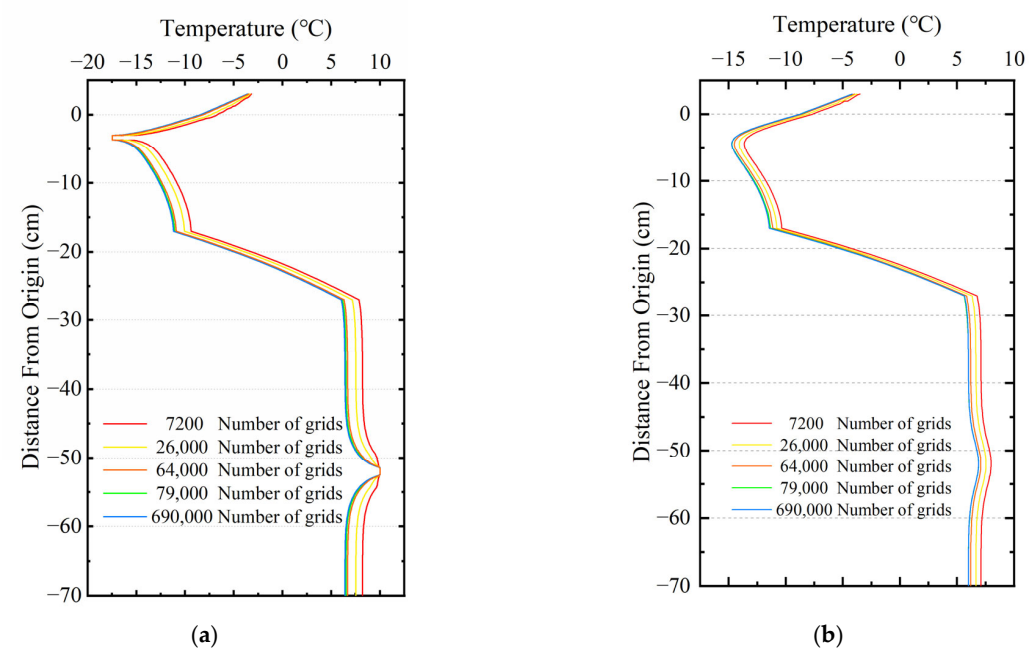


Figure 4. Temperature distribution of different grid numbers: (**a**) Longitudinal Line 1; (**b**) Longitudinal Line 2.

2.4. Model Validation

The experimental results of Li et al. [15] were used to compare and verify the model calculation results. By setting the same physical model and boundary conditions as the experimental environment (ice thickness 60 mm, ice surface temperature −10 °C, water layer thickness 5 mm, water initial temperature 5 °C, ambient temperature 12 °C, heat flux 150 W/m^2), the surface temperature changes under the same conditions were simulated and compared with the corresponding literature data. The verification result of the temperature change is shown in Figure 5. The water temperature variations during the freezing process of the water layer can be divided into three stages: in the first stage, the water has just been laid on the ice surface, the water releases the sensible heat and the temperature falls rapidly, which is called the water sensible heat release stage. In the second stage, when the water temperature drops to about 0 °C, the water solidifies into ice and starts to release the latent heat. The temperature decreases slowly in this stage, which is called the water-ice mixture latent heat release stage. In the third stage, when most of the water has been converted into ice, and the ice releases the sensible heat, the temperature will decline rapidly initially. Until the ice surface temperature is stable, the cooling capacity of the cooling pipe and the heat fluxes on the ice surface reach a balance, which is called the ice sensible heat release stage. It implies that the ice grows mainly in the second stage. It can be found that the first stage is in good agreement. In the second stage, the experimental data are kept at about −0.5 °C, while the simulation data are kept at about 0 °C. This is because the critical temperature of the selected apparent heat capacity method is set at 0 °C, so the freezing process is at about 0 °C. The selection of this critical temperature and temperature range is consistent with [20]; although the temperature has some deviation, the time of the second stage is

basically consistent with the experimental results; the third stage is due to the influence of the thermal physical properties of concrete. There is a deviation between the simulation results and the experiment data in the cooling process, but the time and temperature when the temperature drops to a stable level are not much different from the experimental results. After 120 min, the experimental data and simulation results are stable to about −10 °C. In general, the numerical results can accurately reflect the temperature changes in the whole freezing process.

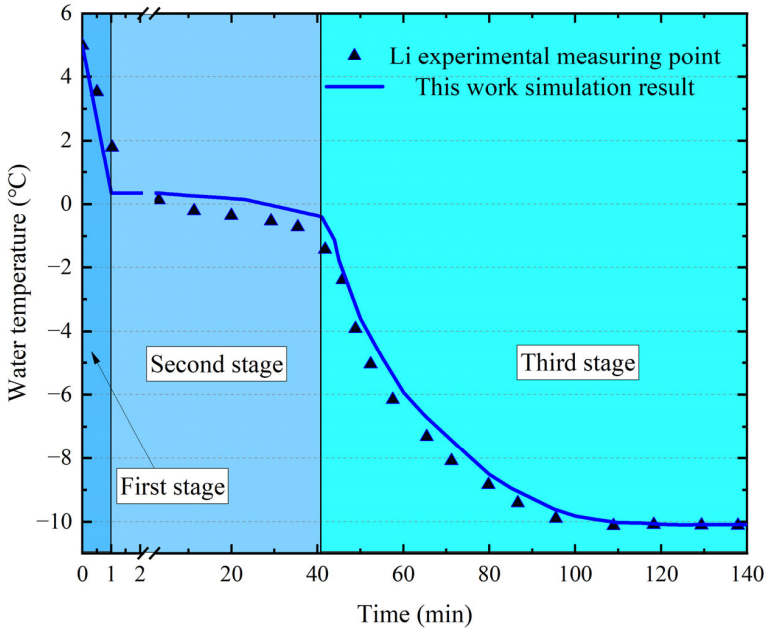


Figure 5. Comparison between model results and experimental results.

3. Results and Discussion

Based on the above-mentioned model, the ice-growing process mainly occurs in the second stage. This paper first analyzes the ice-growing process, including the temperature variations of the water layer and the ice thickness variations of the layer. Then, the influence of water layer thickness, ice surface heat fluxes, cooling pipe arrangement and temperature, and the top-layer concrete thickness on the ice-making process is discussed. Unless otherwise specified, the basic ice rink parameters are assumed to be as follows: the initial temperature of the water is 10 °C, the fluid temperature in cooling pipes is −17.5 °C, the cooling pipe spacing is 50 mm, the surface heat flux is 290 W/m^2 [12], and the 5 mm water layer is frozen [20,26].

3.1. Ice Growing Process

The variations in ice thickness and temperature of the water layer with time are shown in Figure 6. In the initial phase, the whole surface is liquid and there is no ice. The temperature of the water layer gradually decreases with time, and the freezing phenomenon begins to appear. The ice layer thickness is close to 1 mm and the temperature attains −0.3 °C in the 10th minute. With the accumulation and growth of ice, the growth rate of the ice layer continues to slow down, and the thickness of the ice layer increases to 4 mm in the 117th minute. The thickness of the ice layer is close to 5 mm in the 130th minute, and the temperature difference in the investigated layer is about 2.3 °C at the end of the freezing process. It only takes 13 min for the last 1 mm of water to freeze into ice, which implies that the freezing rate is accelerated. This is because most of the water layer has been frozen to ice, and the thermal conductivity of ice is far higher than that of water.

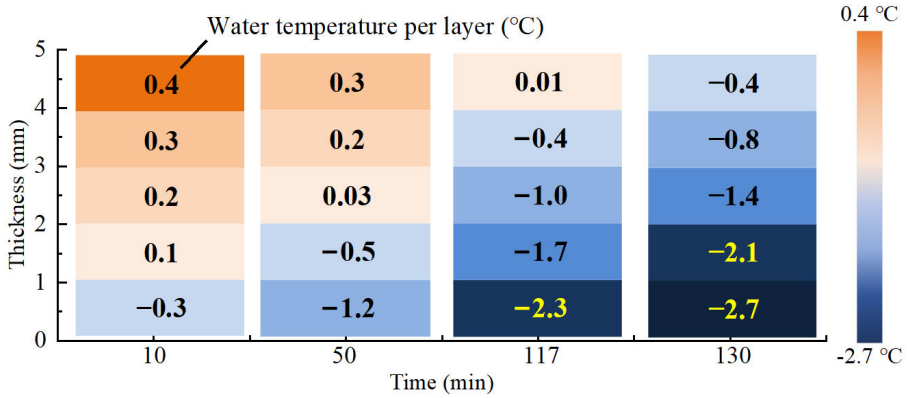


Figure 6. Variations of ice thickness and temperature of the water layer with time.

For the water layer with a thickness of 5 mm, the variations of ice thickness with time are shown in Figure 7. At the initial phase of ice growth (3–15th min), most of the water has not reached 0 °C, and only a small part of the water releases latent heat and converts it into ice. The latent heat release is small, and the surface temperature under the water layer is the lowest. Thus the frozen thickness increases rapidly. At the middle phase of ice growth (15–120th min), most of the water releases latent heat and freezes into ice. The frozen thickness growth results in the increase in the lower surface temperature of the left water layer that is against the ice freezing. Thus the growth rate of the ice layer slows down. The freezing thickness increases almost linearly. At the final phase of ice growth (120–130th min), most of the water has formed ice, and only a small part of the water in the upper layer is left. The thermal conductivity of ice is much greater than that of water, which is conducive to the ice freezing. In addition, the air temperature above the water layer surface becomes lower owing to the continuous cooling. Therefore, the frozen thickness increases more rapidly than in the middle phase. It implies that the time spent in the middle phase accounts for about 80% of the whole ice-growing process. The ice thickness is greatly affected by external factors in the initial and final phases. It is recommended to minimize external heat flux at the initial and final stages of the freezing phase, which is conducive to the freezing of water. The time spent on the ice-growing process can be used to estimate the time of the second stage for engineering reference.

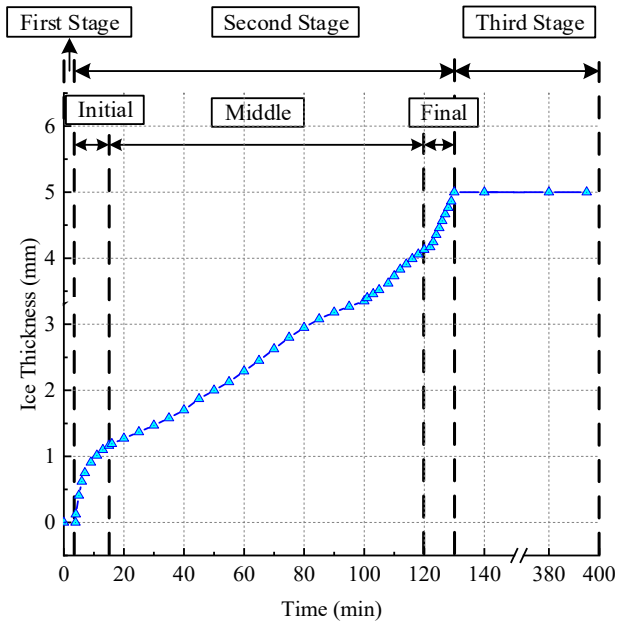


Figure 7. Ice thickness variation with time.

3.2. Effect of Water Layer Thickness

The variation in water layer temperature with time at different water layer thicknesses is shown in Figure 8. It can be seen that the reduction of the water layer thickness is beneficial to accelerating the freezing speed and reducing the final ice temperature. The time of the first stage is 3 min. This means that the temperature of water in contact with ice will drop to the phase transition temperature in a short time. As the thickness of the water layer changes from 3 mm to 7 mm, the time spent on the second stage increases from 55 min to 180 min. The second stage time is increased by 57 min–68 min for every 2 mm thickness increase. When the water layer thickness is 3 mm, 5 mm, and 7 mm, the total time spent on ice-making is about 265 min, 350 min, and 425 min, respectively. It implies that the total time spent on ice-making for the water layer thickness of 3 mm and 5 mm decreases by 37.6% and 17.6%, respectively compared with 7 mm. In addition, with the decrease in the thickness of the water layer, the temperature of the final stable ice layer becomes lower. When the thickness of the water layer is 3 mm, 5 mm, and 7 mm, the temperature of the final ice layer is −5.3 °C, −4.4 °C, and −3.6 °C, respectively. The greater the thickness, the greater the thermal resistance is, resulting in a higher temperature of the stable ice layer.

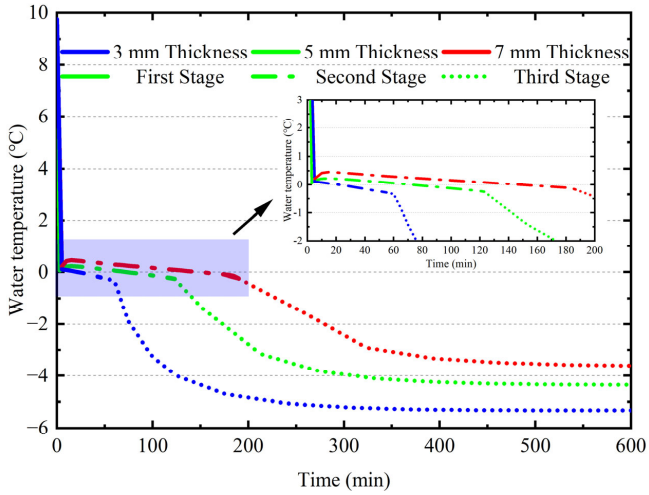


Figure 8. Effect of water layer thickness on water temperature.

3.3. Effect of Water Layer Surface Heat Flux

The variations in conditions above the water surface, such as lighting, air temperature, and velocity, will cause changes in the heat fluxes on the surface. The variation in water layer temperature with time at different water layer surface heat fluxes is shown in Figure 9. In this paper, three heat fluxes of 250 W/m^2, 290 W/m^{2,} and 330 W/m^2 are selected to analyze the ice-making process. With the increase in heat fluxes, the time spent in the first stage increases, and the time spent in the first stage for the three heat fluxes (250 W/m^2, 290 W/m^{2,} and 330 W/m^2) are 42 min, 48 min, and 66 min, respectively. When the surface heat flux is 250 W/m^2, 290 W/m^{2,} and 330 W/m^2, respectively, the time spent in the second stage is 60 min, 120 min, and 230 min, respectively. Under the three heat flux conditions, the total time spent on ice-making is 340 min, 350 min, and 410 min, respectively. It implies that the total time spent on ice-making for the ice surface heat flux of 250 W/m^2 and 290 W/m^2 decreases by 17.1% and 14.6%, respectively compared with 330 W/m^2. It can also be seen that the lower the ice surface heat flux, the lower the temperature of the final stable ice layer. When the surface heat flux is 250 W/m^2, 290 W/m^{2,} and 330 W/m^2 respectively, the temperature of the final ice layer is −6.3 °C, −4.5 °C, and −2.6 °C, respectively. The temperature will decrease by about 1.8 °C for every 40 W/m^2 decrease in the heat flux. As the water layer surface heat flux decreases, the heat obtained by the top water layer becomes less, which is conducive to the water freezing. Moreover, with the decrease in the water surface heat flux, the ice surface temperature will be reduced, which will also

accelerate the freezing process and reduce the final ice temperature. Thus the total time spent on ice-making and the final temperature of the stable ice layer decrease with the reduction in the water layer surface heat flux.

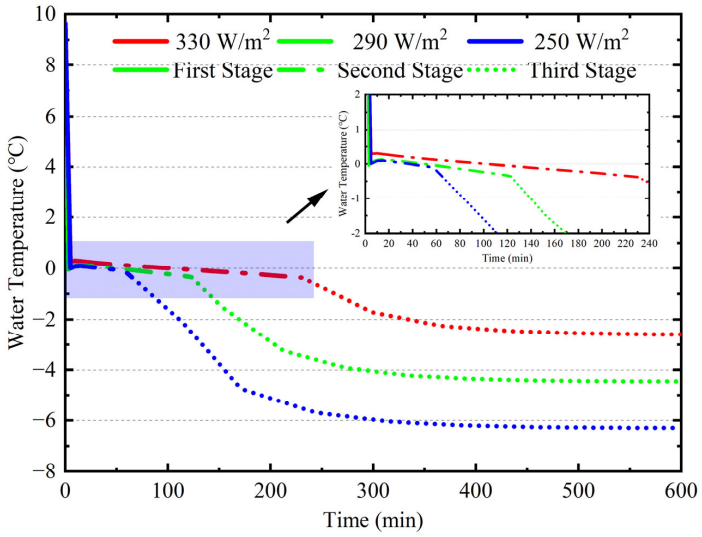


Figure 9. Effect of water layer surface heat flux on water temperature.

3.4. Effect of Cooling Pipe Parameters

The variation in water layer temperature with time at different cooling pipe spacing is shown in Figure 10. The cooling pipe spacing has little effect on the time spent in the first stage of ice-making. When the cooling pipe spacing was reduced from 55 mm to 45 mm, the time spent in the second stage decreased from 130 min to 108 min. For the cooling pipe spacing of 55 mm, 50 mm, and 45 mm, the total time spent on ice-making is 390 min, 350 min, and 345 min, respectively. It implies that the total time spent on ice-making for the cooling pipe spacing of 45 mm and 50 mm decreases by 11.5% and 10.3%, respectively compared with 55 mm. As the cooling pipe spacing decreases from 55 mm to 45 mm, the final temperature of the stable ice layer decreases from −4.1 °C to −4.7 °C. With the reduction in the cooling pipe spacing, the number of cooling pipes increases, leading to an increase in the cooling capacity and the temperature difference between the water layer and the ice surface, which is beneficial to accelerate the ice-making process and reduce the final ice temperature. Thus the total time spent on ice-making and the final temperature of the stable ice layer decrease with the reduction in the cooling pipe spacing.

The variation in water layer temperature with time at different cooling pipe temperatures is shown in Figure 11. It can be seen that a lower cooling pipe temperature can accelerate the freezing rate and reduce the final ice layer temperature. When the fluid temperature in the cooling pipe is −19.5 °C, −17.5 °C, and −15.5 °C, the second stage takes 65 min, 120 min, and 235 min, respectively, the total time spent on ice-making is 330 min, 350 min, and 420 min, respectively. It implies that compared with −15.5 °C, the total time spent on ice-making was shortened by 16.7% and 21.4% for the cooling pipe temperature of −19.5 °C and −17.5 °C, respectively. As the cooling pipe temperature decreases from −15.5 °C to −19.5 °C, the final temperature of the ice layer after stabilization decreases from −2.4 °C to −6.4 °C. The decrease in the cooling pipe temperature implies that more cooling capacity is supplied to the water layer and a higher temperature difference between the water layer and the cooling pipe surface. Thus the total time spent on ice-making and the final temperature of the stable ice layer decreases with the reduction in the cooling pipe temperature.

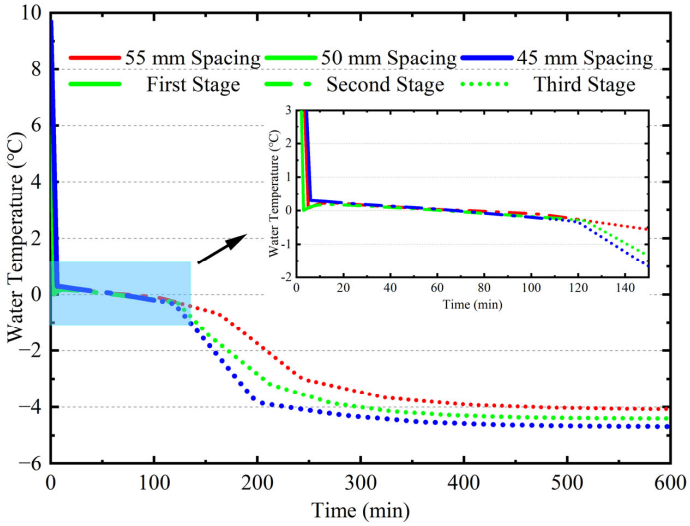


Figure 10. Effect of cooling pipe spacing on water temperature.

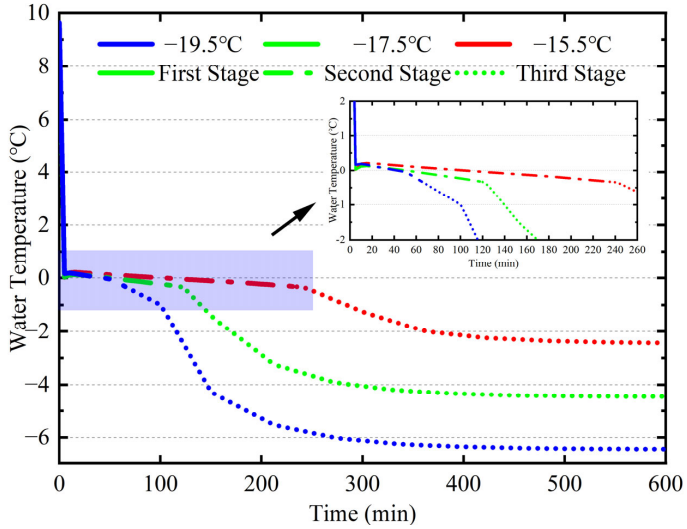


Figure 11. Effect of cooling pipe temperature on water temperature.

3.5. Effect of Top Concrete Thickness

The concrete layer (about 100–150 mm) is embedded with the cooling pipes. The concrete layer is divided into two sub-layers, namely, below and above the cooling pipes. The below concrete layer is to ensure the stability and strength of the structure. And a thinner concrete layer is laid above the cooling pipes, which is called as top concrete here [27]. The variation in water layer temperature with time at different top concrete layer thicknesses is shown in Figure 12. It can be seen that the influence of top concrete layer thickness on the freezing process is mainly in the second stage. With the decrease in thickness from 30 mm to 25 mm, the time spent on the second stage decreases from 123 min to 111 min. The total time spent on ice-making decreases from 350 min to 305 min, with a decrease of 12.9%. As the top concrete layer thickness decreases from 30 mm to 25 mm, the final temperature of the ice layer after stabilization decreases from −4.3 °C to −5.1 °C. The decrease in the top concrete thickness results in lower thermal resistance and a higher temperature difference between the water layer and the ice surface, which is beneficial to accelerating the ice-making process and reducing the final ice temperature. Thus the total time spent on ice-making and the final temperature of the stable ice layer decreases with the decrease in the top concrete layer thicknesses.

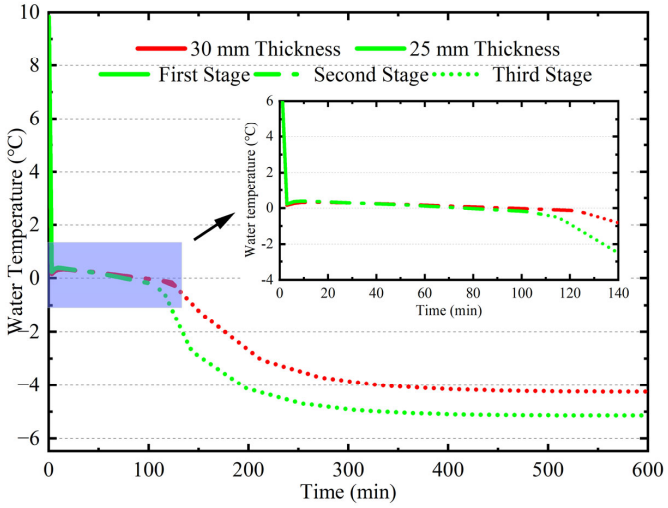


Figure 12. Effect of top concrete thickness on water temperature.

4. Conclusions

In this paper, an unsteady heat transfer model with apparent heat capacity water–ice phase transition is presented for the ice-making process. The simulation results of the model were found to agree well with the experimental measuring results of the cited reference to predict the water layer transient temperature variations. Then, using the validated model, the transient temperature variation and ice thickness growing characteristics during the process are analyzed. The freezing time of the water layer is quantified, and a parametric analysis of the ice rink was performed to identify the influence of the operating conditions and design parameters on the ice-making process.

During the ice-making process, the temperature variation of the water layer mainly goes through three stages: the water sensible heat release stage, the water-ice mixture latent heat release stage, and the ice sensible heat release stage. The growth of ice thickness mainly occurs in the second stage. The total ice-making time and the final temperature of the ice layer after stabilization are significantly affected by the thickness of the water layer, the heat flux on the water layer surface, the spacing of cooling pipes, the fluid temperature in the cooling pipes, and the thickness of the top concrete layer. Among them, the influences of the thickness of the water layer, the surface heat flux, and the fluid temperature in the cooling pipe are more significant. As the thickness of the water layer decreases from 7 mm to 3 mm, the total ice-making time decreases by about 37.6%. The ice-making time is reduced by 17.1% with the surface heat flux decreasing from 330 W/m^2 to 250 W/m^2. The ice-making time is reduced by 21.4% with the cooling pipe temperature decreasing from −15.5 °C to −19.5 °C.

The presented model can be used for the optimization of design parameters of ice to reduce the operating cost of ice rinks. However, the model and this study have potential limitations. Firstly, the water layer surface heat flux was simplified to a fixed value for ease of calculation. In a real ice rink, the air parameters and lighting parameters above the water layer surface change with time, leading to transient variations in surface heat flux, which will affect the ice-making process. Secondly, the temperature difference between the mainstream temperature of the fluid in the cooling pipes and the cooling pipes' outer surface was ignored. Thus, the effect of working fluid in the cooling pipe on the ice-making process cannot be investigated through the current model. In the future, the model can be improved to make it closer to the real ice-making process.

Author Contributions: Conceptualization, Z.Z. and S.W.; methodology, S.W. and Z.Z.; software, S.W. and Y.W.; validation, S.W. and Z.Z.; formal analysis, S.W. and Z.Z.; investigation, S.W. and P.Z.; resources, Z.Z.; data curation, S.W. and Y.W.; writing—original draft preparation, S.W.; writing—review and editing, M.Y. and Z.Z.; visualization, S.W. and H.W.; supervision, Z.Z. and H.W.; project

administration, Z.Z. and M.Y.; funding acquisition, Z.Z. All authors have read and agreed to the published version of the manuscript.

Funding: This research was funded by the S&T Program of Hebei (20474501D), Natural Science Foundation of Hebei Province (E2020209121), Tangshan Science and Technology Innovation Team Training Program (21130202D), and Tangshan Key Laboratory of Low-carbon Built Environment (2022TS002b).

Institutional Review Board Statement: Not applicable.

Informed Consent Statement: Not applicable.

Data Availability Statement: Not applicable.

Conflicts of Interest: The authors declare no conflict of interest.

Nomenclature

Variables	
c	Specific heat capacity [J/(kg·°C)]
h	Convective transfer coefficient [W/(m·°C)]
k	Thermal conductivity [W/(m·K)]
L	Latent heat (kJ/kg)
n	Boundary normal
q	Heat flux (W/m^2)
t	Time (s)
T	Temperature (°C)
∇^2	Laplace operator
Greek	
α	Volume expansion coefficient
ρ	Density (kg/m^3)
θ	Solid-liquid fraction
Subscripts	
0	critical
c	Cooling
i	Ice
p	Constant pressure
v	Internal
w	Water

References

1. Daoud, A.; Galanis, N.; Bellache, O. Calculation of refrigeration loads by convection, radiation and condensation in ice rinks using a transient 3D zonal model. *Appl. Therm. Eng.* **2008**, *28*, 1782–1790. [CrossRef]
2. Rogstam, J.; Karampour, M. *Experimental Cooling Load Analysis of Ice Rinks*, 23rd ed.; International-Institute-of-Refrigeration (IIR) International Congress of Refrigeration: Prague, Czech Republic, 2011.
3. Liu, S. Research on Load of Outdoor Ice Rink Based on CFD Technology. Master's Thesis, Hunan University of Technology, Zhuzhou, China, 2018.
4. Brown, J.; Pearson, S.F. Temperature distribution in ice rink floors. *Aust. Refrig. Air Cond. Heat.* **1983**, *40*, 12–17.
5. Bellache, O.; Ouzzane, M.; Galanis, N. Coupled Conduction, Convection, Radiation Heat Transfer with Simultaneous Mass Transfer in Ice Rinks. *Numer. Heat Transfer Part A Appl.* **2005**, *48*, 219–238. [CrossRef]
6. Bellache, O.; Ouzzane, M.; Galanis, N. Numerical prediction of ventilation patterns and thermal processes in ice rinks. *Build. Environ.* **2005**, *40*, 417–426. [CrossRef]
7. Mun, J.; Krarti, M. Experimental Analysis of Heat Transfer From Ice Rink Floors. In Proceedings of the Asme International Solar Energy Conference, Denver, Colorado, 8–13 July 2006.
8. Somrani, R.; Mun, J.; Krarti, M. Heat transfer beneath ice-rink floors. *Build. Environ.* **2008**, *43*, 1687–1698. [CrossRef]
9. Mun, J. Analysis of Heat Transfer through Ice Rink Floors. Ph.D. Thesis, University of Colorado at Boulder, Boulder, CO, USA, 2010.
10. Coman, G.; Uzuneanu, K.; Dragan, M.; Damian, V. The Temperature Distribution in an Ice Rink Pad. *Termotehnica J.* **2013**, *2*, 144–147.
11. Zhou, W.; Gan, Z.; Han, L. Simulation of the Optimal Refrigerated Floor Design for Ice Rinks. *Energies* **2021**, *14*, 1535. [CrossRef]
12. Zhang, Z.; Wang, S.; Yang, M.; Gong, K.; Chen, Y. Parametric Evaluation of Cooling Pipe in Direct Evaporation Artificial Ice Rink. *Energies* **2022**, *15*, 7989. [CrossRef]

13. Seghouani, L.; Daoud, A.; Galanis, N. Prediction of yearly energy requirements of indoor ice rinks. *Energy Build.* **2008**, *41*, 500–511. [CrossRef]
14. Li, L.; Lin, W.; Zhang, T.; Liu, X. On-site measurement of thermal environment and heat transfer analysis in a curling arena. *J. Build. Eng.* **2020**, *34*, 101691. [CrossRef]
15. Li, L.; Liu, X.; Zhang, T. Investigation of heat and mass transfer characteristics in the ice rink: Ice making, maintaining and resurfacing processes. *Build. Environ.* **2021**, *196*, 107779. [CrossRef]
16. Li, L.; Liu, X.; Zhang, T. Experimental investigation of frosting process on ice surface in ice rink. *Energy Build.* **2022**, *255*, 111671. [CrossRef]
17. Lin, W.; Liu, X.; Li, S.; Zhang, T. Investigation on thermal environment and heat transfer characteristics in ice rinks with different envelopes. *Build. Environ.* **2022**, *219*, 109250. [CrossRef]
18. Lu, Y. *Practical Heating and Air Conditioning Design Manual*; China Construction Industry Press: Beijing, China, 2002.
19. Berno, G.M.; Loyola, F.R.; Hermes, C.J. Comparison between moving-boundary and distributed models for predicting the time evolution of the solidification front in ice trays. *Int. Commun. Heat Mass Transf.* **2020**, *118*, 104711. [CrossRef]
20. Mun, J.; Krarti, M. Optimal insulation for ice rink floors. *Energy Build.* **2015**, *108*, 358–364. [CrossRef]
21. Al-Saadi, S.N.; Zhai, Z. Modeling phase change materials embedded in building enclosure: A review. *Renew. Sustain. Energy Rev.* **2013**, *21*, 659–673. [CrossRef]
22. Voller, V.R. An overview of numerical methods for solving phase change problems. *Taylor Fr.* **1997**, *1*, 341–380.
23. Faghri, A.; Zhang, Y. *Transport Phenomena in Multiphase Systems*; Elsevier Academic Press: San Diego, CA, USA, 2006; pp. 107–176.
24. Wang, B. Application Research on Refrigeration Systems of Ice Rinks With CO_2 as Refrigerant. Master's Thesis, Harbin Institute of Technology, Harbin, China, 2018.
25. Liu, X. Study on Heat Transfer and Refrigeration System of Ice Rink Using CO_2 as Coolant. Master's Thesis, North China University of Science and Technology, Tangshan, China, 2021.
26. Yuan, B. *Research and Application of Artificial Ice Failure Criteria in Ice Rink*; Harbin Institute of Technology: Harbin, China, 2021.
27. Haghighi, E.B.; Makhnatch, P.; Rogstam, J. Energy Saving Potential with Improved Concrete in Ice Rink Floor Designs. *Int. J. Civ. Environ. Struct. Constr. Archit. Eng.* **2014**, *8*, 635–640.

Disclaimer/Publisher's Note: The statements, opinions and data contained in all publications are solely those of the individual author(s) and contributor(s) and not of MDPI and/or the editor(s). MDPI and/or the editor(s) disclaim responsibility for any injury to people or property resulting from any ideas, methods, instructions or products referred to in the content.